THE JOURNAL OF BIOLOGICAL CHEMISTRY VOL. 287, NO. 45, pp. 37659–37672, November 2, 2012
© 2012 by The American Society for Biochemistry and Molecular Biology, Inc. Published in the U.S.A.

Dynamin Regulates Specific Membrane Fusion Events Necessary for Acrosomal Exocytosis in Mouse Spermatozoa

Received for publication, June 18, 2012, and in revised form, August 15, 2012 Published, JBC Papers in Press, September 12, 2012, DOI 10.1074/jbc.M112.392803

Andrew T. Reid[‡], Tessa Lord[‡], Simone J. Stanger[‡], Shaun D. Roman[‡], Adam McCluskey[§], Phillip J. Robinson[¶], R. John Aitken[‡], and Brett Nixon[‡1]

From the [‡]School of Environmental and Life Sciences, Discipline of Biological Sciences and the [§]School of Environmental and Life Sciences, Discipline of Chemistry, The University of Newcastle, University Drive, Callaghan, New South Wales 2308, Australia, and the [¶]Children's Medical Research Institute, Westmead, The University of Sydney, New South Wales 2145, Australia

Background: Mammalian fertilization is preceded by sperm acrosomal exocytosis.
Results: The GTPases, dynamin 1 and 2, were identified within the periacrosomal region of the mouse sperm head and shown to participate in a progesterone-induced acrosome reaction.
Conclusion: Dynamin forms part of the molecular machinery that underpins acrosomal exocytosis.
Significance: These data provide an important mechanistic insight into the molecular basis of the sperm acrosome reaction.

Mammalian spermatozoa must complete an acrosome reaction prior to fertilizing an oocyte. The acrosome reaction is a unique exocytotic event involving a series of prolonged membrane fusions that ultimately result in the production of membrane vesicles and release of the acrosomal contents. This event requires the concerted action of a large number of fusion-competent signaling and scaffolding proteins. Here we show that two different members of the dynamin GTPase family localize to the developing acrosome of maturing mouse germ cells. Both dynamin 1 and 2 also remain within the periacrosomal region of mature mouse spermatozoa and are thus well positioned to regulate the acrosome reaction. Two pharmacological inhibitors of dynamin, dynasore and Dyngo-4a, blocked the *in vitro* induction of acrosomal exocytosis by progesterone, but not by the calcium ionophore A23187, and elicited a concomitant reduction of *in vitro* fertilization. *In vivo* treatment with these inhibitors also resulted in spermatozoa displaying reduced acrosome reaction potential. Dynamin 1 and 2 phosphorylation increased on progesterone treatment, and this was also selectively blocked by dynasore. On the basis of our collective data, we propose that dynamin could regulate specific membrane fusion events necessary for acrosomal exocytosis in mouse spermatozoa.

The dynamin family of proteins are a novel group of GTPases that have been the focus of intense research since their discovery in the late 1980s (1). The interest in this family stems from their unique ability to manipulate membrane vesicles, not only as a part of endocytosis (scission) but also in regulating particular aspects of post-Golgi vesicle exocytosis (2–4). Three classical dynamin proteins, arising from three unique genes, are known to be present in mammals: dynamin 1 is regarded as the form mainly present in cells of the central nervous system, dynamin 2 is ubiquitously expressed throughout the body (5), and dynamin 3 is expressed chiefly in the testis and brain (6). Although many studies investigating the expression and function of the three classical dynamins have been conducted in somatic cells/tissues, to date there are only a handful of equivalent studies within male germ cells.

Apart from studies focusing on the testis, to the best of our knowledge only two studies have examined dynamin expression in spermatozoa. In the rat, dynamin 3 has been localized to a highly restricted region at the connecting piece of mature sperm that does not correspond with the acrosome, and it also associates with tubulobulbar complexes in the germinal epithelium (7). Dynamin 2 has been shown to specifically localize to the acrosomal cap in mature murine spermatozoa (8); however, other dynamins were not examined in this study, and the possible presence of dynamin 1 in mouse sperm has not been evaluated. Within the acrosome, dynamin 2 interacts with complexins I and II (8). The complexins themselves are known to bind members of the SNARE (soluble *N*-ethylmaleimide-sensitive factor attachment protein receptor) family (9), thus raising the possibility that dynamin 2 may have a role in the events necessary for the acrosome reaction in mature spermatozoa.

The acrosome reaction is an exocytotic event in which the contents of the acrosome, a large secretory vesicle that surrounds the compact nucleus of the spermatozoon, are released. This process may occur at the surface of the zona pellucida or even earlier, as the spermatozoa are approaching the egg during their penetration of the cumulus mass (10). Wherever it occurs, the acrosome reaction is widely acknowledged as a prerequisite for successful fertilization *in vivo*, and failures in this process have been identified as a significant cause of human infertility (11). Unlike traditional exocytosis, which is an extremely rapid process, the acrosome reaction is much slower in its execution. It occurs as a result of multiple fusion events between the outer acrosomal membrane and plasma membrane of the spermatozoon, resulting in the formation of mixed vesicles (12, 13). The released acrosomal contents then digest a path through the zona pellucida, allowing spermatozoa access to the egg plasma membrane. In addition, the acrosome reaction may be involved in remodeling the sperm surface in preparation for sperm-oocyte fusion.

[1] To whom correspondence should be addressed: School of Environmental and Life Sciences, Discipline of Biological Sciences, University of Newcastle, University Drive, Callaghan, NSW 2308, Australia. Tel.: 61-2-4921-6977; Fax: 61-2-4921-6308; E-mail: Brett.Nixon@newcastle.edu.au.

For spermatozoa to respond to the cumulus-oocyte complex by undergoing the acrosome reaction, these cells must have first have completed a final maturation process in the female reproductive tract known as "capacitation" (14, 15). This process is initiated by a rise in intracellular calcium that triggers a signal transduction pathway resulting in a global increase in tyrosine phosphorylation (16, 17). A second increase in cytosolic Ca^{2+} then occurs as spermatozoa engage the cumulus-oocyte complex and is mediated by voltage-dependent and store-operated channels that promote a major Ca^{2+} surge, leading to acrosomal exocytosis (18, 19).

An interesting consequence of the Ca^{2+} influx that occurs during sperm-egg interaction is the disassembly of SNARE proteins from their *cis*-complex state and reassembly into a *trans*-configuration. The assembly of SNARE proteins in their *trans*-state appears to prime the sperm and enables them to respond the final Ca^{2+} surge by undergoing the multiple membrane fusions that are essential for the acrosome reaction (20). Members of the dynamin family are known to interact with a number of proteins important in the highly regulated processes of synaptic vesicle exocytosis (21–23). In addition to their association with such proteins, it is also becoming more apparent that dynamin and dynamin-like GTPases play functional roles not only in membrane fission, but also in membrane fusion (23–25). In view of the importance of dynamin in a number of endo/exocytotic processes that parallel the membrane manipulation events required during acrosomal exocytosis, we hypothesize that dynamin may fulfill a distinct functional role in the sperm acrosome reaction. In this study we have characterized the presence of the three mammalian classical dynamins: 1, 2, and 3, throughout the maturation of mouse spermatozoa. Through the use of specific pharmacological inhibition (dynasore and Dyngo-4a^{TM} (26)), we have also sought to investigate the functional role of dynamin in regulation of the acrosome reaction. The results of our study provide the first direct evidence in support of a functional role of dynamin in the promotion of this highly specialized exocytotic process.

EXPERIMENTAL PROCEDURES

Animals—All of the experimental procedures were carried out with the approval of the University of Newcastle's Animal Care and Ethics Committee. The mice were obtained from a breeding colony held at the institute's Central Animal House and maintained according to the recommendations prescribed by the Animal Care and Ethics Committee. The mice were housed under a controlled-lighting regime (16 of light and 8 h of dark) at 21–22 °C and supplied with food and water *ad libitum*. Prior to dissection, the animals were killed via CO_2 inhalation.

Antibodies and Reagents—Unless otherwise stated, the chemicals were purchased from Sigma and were of molecular biology or research grade. Rabbit polyclonal antibodies against dynamin 1, sheep polyclonal Ser-774 phosphorylated dynamin 1 (Dnm1p774), and Ser-778 phosphorylated dynamin 1 (Dnm1p778) were generated in our laboratory as previously described (27). Phospho-specific antibodies to Ser(P)-774 and Ser(P)-778 were raised in sheep against synthetic phosphopeptides PAGRRS*PTSC and CTSS*PTPQR, respectively (where the S* represents Ser(P)) (27). Goat polyclonal antibody against dynamin 2 was purchased from Santa Cruz Biotechnology (Santa Cruz, CA). Rabbit polyclonal antibody against dynamin 3 was purchased from ProteinTech Group (Chicago, IL). Rat polyclonal antibody against germ cell nuclear antigen (GCNA)[2] was a kind gift from George Enders (28). Anti-rabbit IgG-HRP was from Upstate Biotechnology (Lake Placid, NY), and anti-goat IgG-HRP was from Calbiochem (Darmstadt, Germany). Alexa Fluor 488-conjugated goat anti-rabbit, Alexa Fluor 488-conjugated donkey anti-goat IgG, and Alexa Fluor 594 goat anti-rat were from Invitrogen (Mount Waverley, Victoria, Australia). Anti-goat IgG-FITC and anti-rabbit IgG-FITC were purchased from Santa Cruz Biotechnology. Hepes, penicillin, and streptomycin were obtained from Invitrogen. BSA was obtained from Research Organics (Cleveland, OH). Minicomplete protease inhibitor mixture tablets were from Roche Applied Science. Nitrocellulose was from Amersham Biosciences. Mowiol 4-88 was from Calbiochem (La Jolla, CA), and paraformaldehyde was supplied by ProSciTech (Thuringowa, Australia). Dynasore was purchased from Tocris Bioscience. The dynamin inhibitor Dyngo-4a was generated in our laboratory as previously described (29). Dynasore and Dyngo-4a inhibit dynamin through binding an allosteric site in the GTPase domain of dynamin 1 and 2. Dyngo-4a^{TM} and Dyngo^{TM} are trademarks of Newcastle Innovation Ltd. and Children's Medical Research Institute and are available from Ascent Scientific Ltd. (Bristol, UK). Dynamin 2 was expressed and purified as described previously (30). The same method was used to express and purify full-length wild-type dynamin 1 and 3 (both human sequence). Equine chorionic gonadotropin and human chorionic gonadotropin were obtained from Intervet (Sydney, Australia).

Preparation of Spermatozoa and Early Germ Cells—Populations of capacitated and noncapacitated spermatozoa were prepared following collection from the cauda epididymides of adult male mice (>8 weeks old) as previously described (31, 32). Capacitation, as defined by hyperactivation, zona binding, and, critically the ability to acrosome react has been previously shown under these conditions (32, 33). Following collection, sperm concentration was determined, and the cells diluted as required. Sperm were then assessed for motility, and the noncapacitated samples were used immediately. Alternatively, populations of capacitated spermatozoa were prepared by incubation for 45 min at 37 °C under an atmosphere of 5% CO_2, 95% air. At regular intervals throughout the incubation, sperm suspensions were gently mixed to prevent settling of the cells, and at the end of the incubation, sperm vitality and motility were again assessed. Neither parameter was affected by any of the treatments reported in this study. To prepare caput spermatozoa, the caput region of the epididymis was dissected and placed in a droplet of Biggers, Whitten, and Whittingham medium (34). Several incisions were then made in the tissue, and spermatozoa were gently teased out into medium with mild agitation. The resultant cell suspension was then layered over a

[2] The abbreviations used are: GCNA, germ cell nuclear antigen; TRITC, tetramethylrhodamine isothiocyanate; PL, phospholipase; PNA, peanut agglutinin; BAPTA-AM, 1,2-bis-(*o*-aminophenoxy)-ethane-*N*,*N*,*N*′,*N*′-tetraacetic acid-tetrakis(acetoxymethyl ester).

27% Percoll gradient and subjected to centrifugation at 400 × *g* for 15 min. A population of approximately 95% pure caput spermatozoa was obtained from the pellet, and these cells were then gently washed (400 × *g* for 2 min) in Biggers, Whitten, and Whittingham medium to remove excess Percoll. The cells were then used for immunofluorescence as described below.

Enriched populations of early germ cells were prepared from mouse testes using previously described procedures (35). Briefly, following dissection and dissociation of the testes spermatogonia, pachytene spermatocytes and round spermatids were isolated by density gradient sedimentation on a 2–4% continuous BSA gradient (35). The purity of these samples typically exceeds 90% for spermatogonia, 65–70% for spermatocytes, and 85–95% for round spermatids.

SDS-PAGE and Western Blotting—Proteins were extracted from mature spermatozoa, as well as homogenized brain tissue (positive control), in SDS extraction buffer (0.375 M Tris, pH 6.8, 2% w/v SDS, 10% w/v sucrose) containing protease inhibitor mixture via incubation at 100 °C for 5 min. The protein extracts were centrifuged at 17,000 × *g* for 10 min at 4 °C to remove insoluble material, and soluble proteins were quantified using BCA protein assay kit (Thermo Scientific). The proteins were boiled in SDS-PAGE sample buffer (2% v/v mercaptoethanol, 2% w/v SDS, and 10% w/v sucrose in 0.375 M Tris, pH 6.8, with bromphenol blue) and resolved by SDS-PAGE on polyacrylamide gels followed by transfer onto nitrocellulose membranes. The membranes were blocked with 3% w/v BSA (dynamin 1, dynamin 1 p774, dynamin 1 p778 and dynamin 3) or 5% w/v skim milk powder (dynamin 2) in TBS, pH 7.4) for 1 h before being probed with primary antibody (1:1,000 dynamin 1, dynamin 1 p774, dynamin 1 p778; 1:250 dynamin 2; 1:500 dynamin 3) in TBS containing 1% w/v BSA or 1% w/v skim milk powder and 0.1% v/v polyoxyethylenesorbitan monolaurate (Tween 20; TBS-T) overnight at 4 °C. The blots were washed three times in TBS-T followed by incubation with appropriate HRP-conjugated secondary antibodies (diluted 1:1,000 in TBS-T) for 1 h. Following three additional washes in TBS-T, proteins were detected using an enhanced chemiluminescence kit (Amersham Biosciences).

Immunofluorescent Localization of Dynamin Isoforms—Mouse testis and epididymal tissue were paraformaldehyde fixed, embedded in paraffin, and sectioned onto slides (5 μm). Embedded tissue was dewaxed and rehydrated before being subjected to antigen retrieval via immersion in 10 mM sodium citrate (pH 6.0) and microwaving for 3 × 3 min at 1,000 W. All of the subsequent incubations were performed at 37 °C in a humid chamber, and all antibody dilutions and washes were conducted in PBS. The sections were blocked using either 10% v/v whole goat serum (dynamin 1 and 3) or 10% v/v whole donkey serum (dynamin 2) supplemented with 3% w/v BSA in PBS for 1 h. The slides were rinsed and incubated with antibodies diluted 1:100 (dynamin 1) or 1:50 (dynamin 2 and 3) overnight at 4 °C. The slides were washed three times followed by incubation in appropriate Alexa Fluor 488-conjugated secondary antibodies (1:200) for 1 h at room temperature. The sections were then washed and incubated with the nuclear counterstain propidium iodide (2 mg/ml). Following washes, the slides were mounted using anti-fade reagent (13% Mowiol 4-88, 33% glycerol, 66 mM Tris, pH 8.5, 2.5% 1,4-diazabicyclo-[2.2.2]octane) and viewed under an LSM510 laser scanning confocal microscope (Carl Zeiss Pty, Sydney, Australia). Germ cell stages were identified according to their developing acrosome morphology as classified in Ref. 36.

For immunofluorescence in cells, isolated germ cells were fixed in 2% w/v paraformaldehyde and washed three times in PBS containing 0.05 M glycine. Fixed cells were aliquoted onto poly-L-lysine-coated slides and air-dried before being permeabilized in ice-cold methanol for 10 min. All of the subsequent incubations were performed at 37 °C in a humid chamber, and all antibody dilutions and washes were conducted in PBS. The cells were blocked, washed, and incubated in primary antibody as per tissue protocol. After washing, the cells were incubated in appropriate FITC-conjugated secondary antibodies for 1 h. These were again washed and counterstained using TRITC-labeled peanut agglutinin (PNA) (1 μg/μl) for 20 min. For spermatogonia, the cells were coincubated at 4 °C overnight in the primary antibodies against both dynamin and GCNA (1:10), followed by washing and incubation in appropriate secondary antibodies for each dynamin. The slides were then washed and incubated in secondary antibody for GCNA (1:200) for 1 h and counterstained in DAPI. Mounting and viewing was performed as per tissue protocol.

Acrosome Reaction Assays—To determine whether dynamin participates in acrosomal exocytosis, spermatozoa were treated with either A23187 (calcium ionophore) or progesterone in the presence of two specific inhibitors of dynamin 1 and 2, Dyngo-4a, and dynasore. Following incubation under appropriate conditions (noncapacitated, capacitated, 0.02% Me_2SO, and dynamin-inhibited (Me_2SO vehicle)) spermatozoa were induced to acrosome react by incubation in either 2.5 μM A23187 for 30 min or 15 μM progesterone for 15 min. Intracellular Ca^{2+} was chelated by incubation of spermatozoa in 10 μM BAPTA-AM for 15 min followed by progesterone addition. Sperm suspensions were then washed, resuspended in hypoosmotic swelling medium, and incubated for an additional 1 h (37). Following incubation, spermatozoa were washed, aliquoted onto 12-well slides, air-dried, and permeabilized by immersion in methanol for 10 min. The slides were then stained with TRITC-labeled PNA (1 μg/μl) for 20 min at room temperature and mounted with 5 μl of antifade reagent, and the acrosomal status of viable cells was examined using a Zeiss Axioplan 2 fluorescence microscope (Zeiss, Jena, Germany).

Effects of Dynamin Inhibitors on in Vitro Fertilization—Six-week-old female mice were injected intraperitoneally with 7.5 IU equine chorionic gonadotropin, followed 48 h later with 7.5 IU human chorionic gonadotropin to promote superovulation. The mice were culled ~14 h after human chorionic gonadotropin treatment, and the ovaries were removed immediately into 37 °C PBS. The cumulus mass was retrieved from the ampullae, and the oocytes were denuded from cumulus cells via 5 min of incubation in hyaluronidase (300 μg/ml). The oocytes were then washed in M2 medium to isolate them from cumulus cells.

For *in vitro* fertilization we utilized a modified protocol based on previous *in vitro* fertilization studies (38). Briefly, the oocytes were washed four times in high calcium human tubal fluid medium (39) and were placed in fertilization medium

(high calcium human tubal fluid containing reduced glutathione (1 mM)). Mouse spermatozoa were prepared as previously described (noncapacitated, capacitated, 10 μM Dyngo-4a-treated, 10 μM dynasore-treated, or Me_2SO vehicle control-treated), and then a suspension of $\sim 2 \times 10^5$ cells were added to fertilization dishes containing oocytes. The gametes were coincubated for 4 h at 37 °C under 5% CO_2. Following fertilization, the oocytes were washed four times in high calcium human tubal fluid (no GSH) and incubated overnight to the two-cell stage. Numbers of two-cell embryos were then counted and expressed as a percentage of total oocytes. Between 30 and 40 oocytes were used for each treatment, and experiments were repeated a minimum of three times.

Effect of Dynamin Inhibitors in Vivo—A dosage regime based upon the study by Harper *et al.* (26) was employed in which a total of 3 mg of either Dyngo-4a (three males) or dynasore (three males) (as well as vehicle control; three males) were each administered via two 1.5-mg (30 mg/kg) intraperitoneal injections spaced at 6-h intervals.

Inhibitors were initially prepared in Me_2SO to the appropriate concentration followed by a 1:1 dilution in sesame oil. After 5 days, the spermatozoa from these animals were assessed for their viability using eosin exclusion (40) and motility via counts of forward progressive motility, as well as their ability to undergo an *in vitro* acrosome reaction. A minimum of 200 cells were assessed in each assay.

Statistical Analysis—All of the experiments were replicated a minimum of three times with pooled semen samples obtained from at least three different male mice. Graphical data are presented as the mean values ± standard error of the mean, being calculated from the variance between samples. Statistical significance was determined using an analysis of variance.

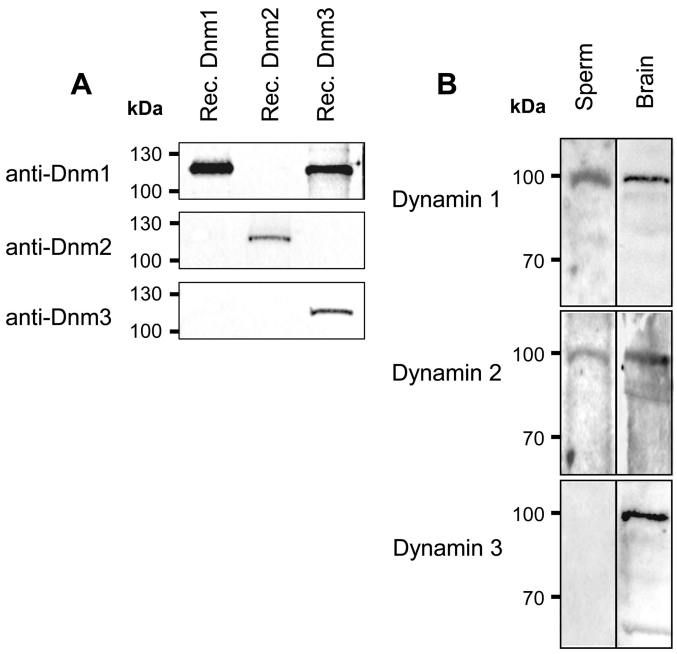

FIGURE 1. **Examination of the specificity of dynamin antibodies.** *A*, recombinant dynamin proteins were overexpressed, isolated, and subjected to SDS-PAGE followed by transferral to nitrocellulose membranes. Each membrane containing recombinant dynamin (*Rec. Dnm*) 1, 2, and 3 was probed with each of the three dynamin antibodies against dynamin 1, 2, and 3 to determine the specificity of each antibody. It is clear that anti-dynamin 1 detects both dynamin 1 and dynamin 3, whereas anti-dynamin 2 and 3 detect a single band corresponding to dynamin 2 and 3, respectively. *B*, identification of dynamin 1 and 2 in mouse spermatozoa. SDS extracted protein from mouse brain homogenates (40 μg) and spermatozoa (40 μg) was separated as above before being probed with antibodies directed against dynamin 1–3. Each blot revealed a predominant band at ~100 kDa, highlighting the presence of all three isoforms in brain positive control, whereas only dynamin 1 and 2 were detected in mature spermatozoa. These experiments were repeated three times using pooled brain and semen samples from at least three mice, and representative immunoblots are shown.

RESULTS

Dynamin 1 and 2 Are Expressed in Mature Mouse Spermatozoa—Prior to use for the characterization of dynamin expression in mouse spermatozoa, the specificity of the three dynamin antibodies used in this study was assessed by immunoblotting against recombinant dynamin protein. As anticipated, each antibody strongly labeled the target protein and, with the exception of anti-dynamin 1, which showed cross-reactivity with dynamin 3, the antibodies appeared to be highly specific and thus suitable for use in the detection of the individual dynamin isoforms (Fig. 1*A*). Using these antibodies, lysates prepared from mouse brain homogenates (positive control) and mature (cauda epididymal) spermatozoa were examined for dynamin expression by immunoblotting (Fig. 1*B*). Specific bands of the expected molecular weight were detected for all dynamins in brain tissue, confirming detection of the three dynamins. These studies also revealed the anticipated presence of a single predominant band at the expected molecular mass of ~100 kDa for dynamin isoforms 1 and 2 within mature spermatozoa. Interestingly, this is the first report of dynamin 1 protein expression in mature mammalian sperm. In contrast to the clear labeling of the appropriate size band in protein extracted from brain, there was no detection of dynamin 3 within mature mouse spermatozoa. This observation is in contrast to a previous report that detected small amounts of dynamin 3 in the connecting piece of rat sperm by immunofluorescence (7). It should be noted that although the antibody raised against dynamin 1 also detects dynamin 3 (Fig. 1*A*), the lack of detection using anti-dynamin 3 indicates the presence of dynamin 1 and not dynamin 3 in mature mouse spermatozoa.

Immunolocalization of Dynamin in Mouse Testis—Following detection of dynamin isoforms 1 and 2 within mature spermatozoa, we next explored the localization of these proteins during spermatogenesis. The results of immunohistochemical studies demonstrated a predominant crescent-shaped localization of dynamin 1 and 2 in maturing germ cells (*arrows*), a pattern that appeared to correspond to that of the developing acrosome (Fig. 2, *A* and *E*). Furthermore, in cells that resembled step 3 to step 5 stage germ cells (36), the localization of dynamin 1 and 2 corresponded to that of the pro-acrosomal vesicle (Fig. 2, *B–D* and *F–H*), implicating these isoforms in acrosomal vesicle formation. A less intense staining pattern that did not correspond to the developing acrosome was also observed proximate to some maturing germ cells for dynamin 1 and 2 (*arrowheads*). In contrast, dynamin 3 exhibited a unique pattern of staining (Fig. 2, *I–L*). No labeling of the developing acrosome was evident; instead, a faint punctate localization pattern was observed within groups of germ cells proximal to the basement membrane, and in advanced stages of maturation, this staining was eventually lost.

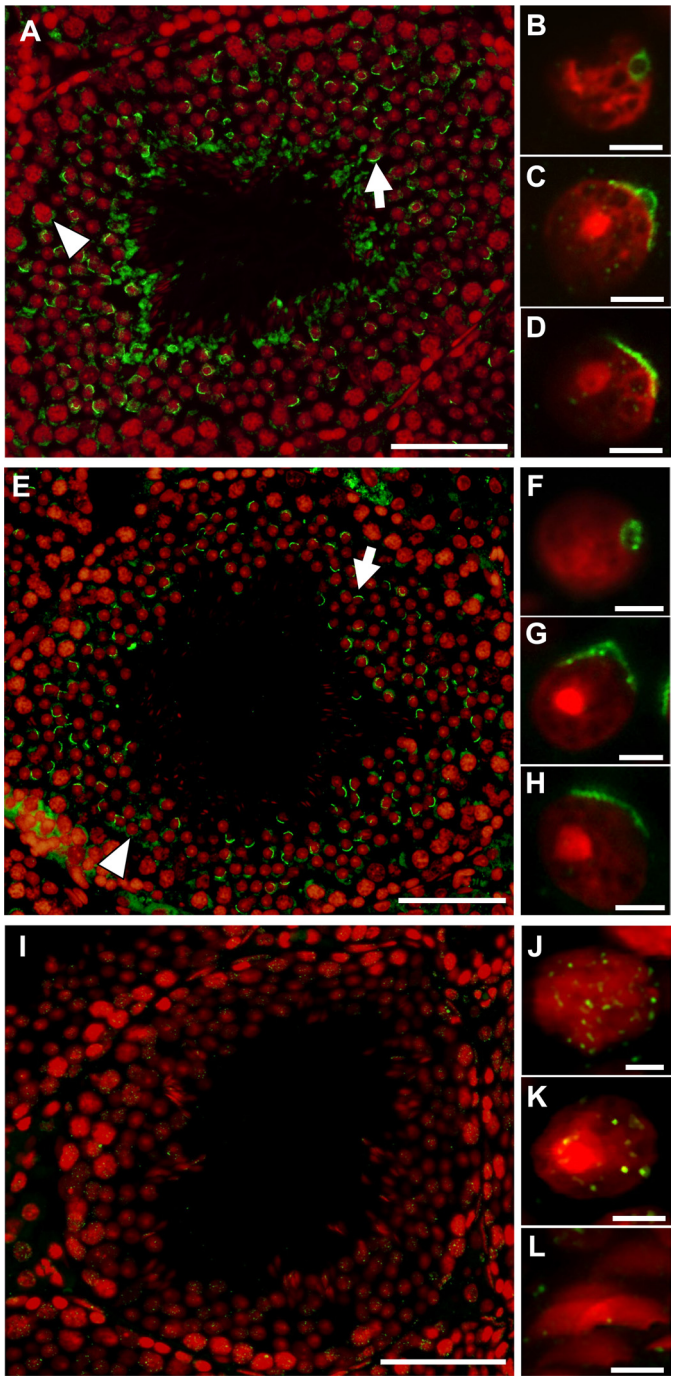

FIGURE 2. **Detection of dynamin isoforms 1–3 within mouse testis.** Mouse testis sections were subjected to immunolocalization with antibodies against dynamin isoforms 1 (*A–D*), 2 (*E–H*), and 3 (*I–L*) (*green*) and counterstained with the nuclear dye, propidium iodide (*red*). Dynamin isoforms 1 and 2 (*A–H*) localized to a structure within maturing germ cells that coincides with the proacrosomal vesicle (*A* and *E*; *arrow*), showing the characteristic flattening as the germ cells mature (*B–D* and *F–H*). A less intense nonacrosomal labeling was also observed for dynamins 1 and 2 proximate to a number of early germ cells (*A* and *E*; *arrowhead*). Dynamin 3 displayed minimum punctate labeling throughout the developing germ cells. The images are representative of entire testis section. *Scale bars*,100 μm for *A*, *E*, and *I*; and 7 μm for *B–D*, *F–H*, and *J–L*.

Immunofluorescent Labeling of Dynamin in Isolated Germ Cells—To refine our analysis of dynamin protein expression, we next aimed to observe the expression patterns for the three dynamin isoforms in isolated germ cells. For this purpose, whole adult mouse testis was subjected to density gradient fractionation to enrich for populations of spermatogonia, pachytene spermatocytes, and round spermatids (35). These cells, along with spermatozoa isolated from the caput region of the epididymis, were assayed using immunofluorescence to localize the three dynamin isoforms (Figs. 3 and 4).

Spermatogonial germ cells were identified in fractionated samples by counterstaining with anti-GCNA, an antibody to an unidentified protein that is abundantly expressed in the nucleus of the cell. The immunocytochemical analysis of this population of cells failed to identify staining for either dynamin 1 or 2, indicating that neither protein was expressed at this early stage of spermatogenesis (Fig. 3, *A* and *B*). In contrast, a punctate staining pattern was observed across the entire cell for dynamin 3 (Fig. 3*C*). This staining may highlight areas of vesicle transport, such as endocytotic hot spots in these early germ cells.

As the germ cells progress through various developmental stages within the testis (pachytene spermatocytes and round spermatids), as well as the first stage of epididymal maturation (caput epididymal sperm), we observed a clear change in the pattern of localization for each of the three dynamins (Fig. 4). Dynamin 1 (*green*) was uniformly detected throughout the majority of isolated pachytene spermatocytes before becoming concentrated within the vicinity of the developing acrosome of round spermatids. Within this region, dynamin 1 showed strong colocalization with PNA, a marker of the outer acrosomal membrane (Fig. 4). Dynamin 2 was initially detected around the periphery of pachytene spermatocytes. However, as these cells reach the round spermatid stage, dynamin 2 becomes confined within the developing acrosome and strongly colocalizes with PNA. In contrast to dynamin 1, very little dynamin 2 was detected beyond the margin of the periacrosomal region. The location of dynamin 2 at this region is consistent with data suggesting that the acrosome of the germ cell arises via a Golgi remodeling event that is mediated by vesicle trafficking (41). The finding that dynamin 1 also localizes strongly to the periacrosomal reaction is surprising and may indicate some functional redundancy between dynamins 1 and 2. A unique pattern of staining was observed for dynamin 3 in isolated germ cells. Similar to the results obtained in spermatogonia (Fig. 3), dynamin 3 staining of isolated pachytene spermatocytes appeared as a series of discrete bright fluorescence spots (Fig. 4). Notwithstanding some minor variation, these spots appeared concentrated around the periphery of the cell at what appears to be the plasma membrane. An observable difference between mouse and rat is that as these cells continue to mature, dynamin 3 is no longer detectable in later stages of development.

Dynamin in Mature Spermatozoa—An intriguing question that arises from the finding that dynamin isoforms 1 and 2 become concentrated within the developing acrosomal region of maturing spermatozoa is whether this reflects participation in the Golgi remodeling events that accompany spermatogenesis and/or whether they are sequestered to this position to fulfill an important functional role in mature spermatozoa. To investigate the latter possibility, we sought to examine whether the proteins are retained in this domain in mature cauda spermatozoa. Both dynamin 1 and dynamin 2 are predominantly

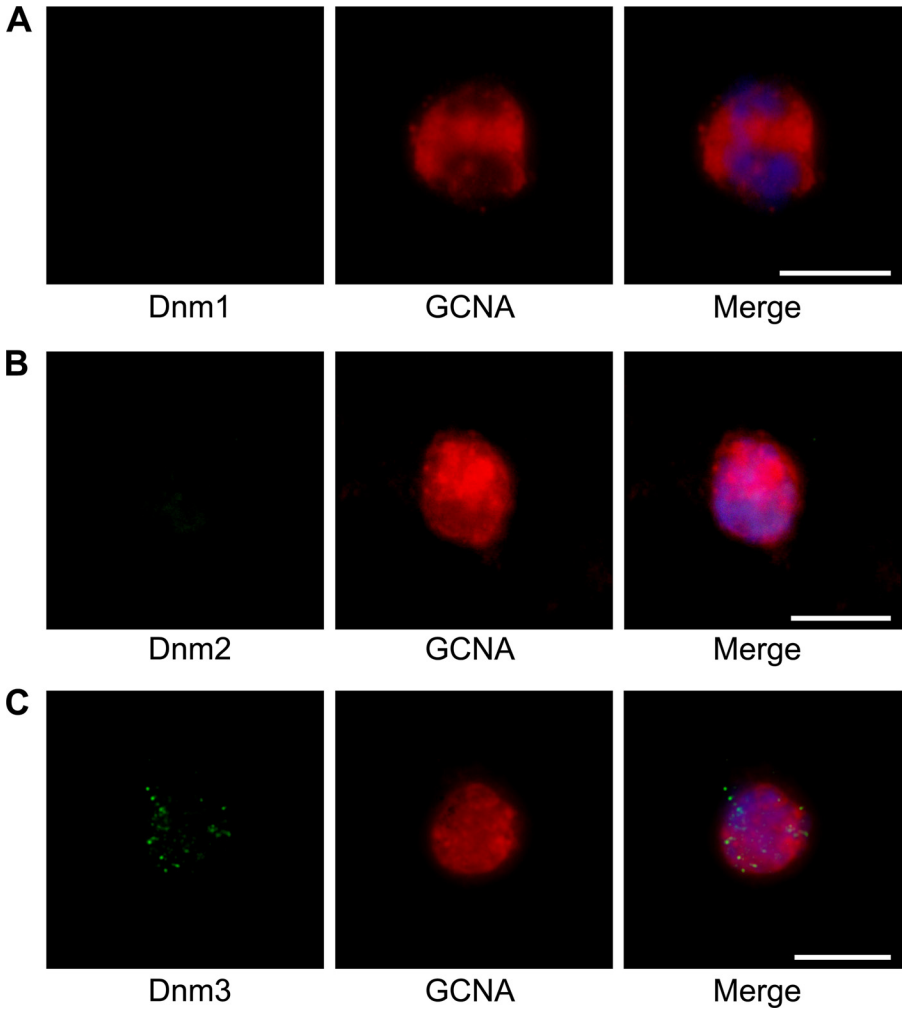

FIGURE 3. **Immunofluorescent staining of isolated spermatogonia labeled for the three dynamin isoforms (*green*), GCNA (*red*), and counterstained using DAPI (*blue*).** Spermatogonia, identified on the basis of positive GCNA labeling, failed to label with either dynamin 1 (*A*) or dynamin 2 (*B*) antibodies. In contrast, dynamin 3 (*C*) antibodies exhibited a distinct punctate localization pattern. The images are representative for the population of spermatogonia. *Scale bars*, 15 μm.

expressed in the periacrosomal region of mature mouse spermatozoa (Fig. 5). As with round spermatids and caput epididymal spermatozoa, both proteins strongly colocalized with PNA in this region, suggesting that they reside proximal to, or within, the outer acrosomal membrane. Although dynamin 2 staining was uniquely restricted within this region, dynamin 1 was also detected around the ventral surface of the sperm head. Dynamin 3 was barely detectable in these cells.

Inhibition of Dynamin 1 and 2 Compromises the Acrosomal Reaction—Given the well characterized roles of dynamin in vesicle trafficking, its most likely role in the periacrosomal region of mature spermatozoa is in the mediation of acrosomal exocytosis. A previous study provided indirect evidence that dynamin 2 may participate in this event (8). Therefore, our next aim was to determine whether dynamin 1 and/or 2 are involved in the acrosome reaction. Through the application of two selective pharmacological inhibitors, we first tested whether the suppression of dynamin GTPase activity is able to inhibit the acrosome reaction. We induced the acrosome reaction in capacitated sperm populations by two approaches: a calcium ionophore (A23187, 2.5 μM) or progesterone challenge (15 μM), in the presence or absence of the membrane permeable, small molecule inhibitors of dynamin, dynasore (IC_{50} = ~15 μM) (42), and Dyngo-4a (IC_{50} = 0.38 μM for dynamin 1 and 2.6 μM for dynamin 2) (26) at various concentrations. Both inhibitors are known to act upon the GTPase domain of dynamin 1 and 2. Neither inhibitor compromised sperm viability or motility even at the highest concentrations used in this study (data not shown). After preincubation with the dynamin inhibitors, the cells were stimulated with either A23187 or progesterone (43), followed by the simultaneous assessment of cell viability and acrosomal status. As anticipated, there was a highly significant increase in the number of acrosome-reacted cells in capacitated and vehicle (capacitated + 0.02% Me_2SO) controls when compared with noncapacitated spermatozoa (Fig. 6). Because of distinct modes of action for progesterone and A23187, we generally observed more acrosome-reacted spermatozoa with A23187 compared with progesterone (Fig. 6). Interestingly, the A23187 induced acrosome reaction proved resistant to dynamin inhibitors, even at concentrations ~10-fold greater than the IC_{50} values for inhibition of dynamin GTPase activity (Fig. 6*A*). In marked contrast, both dynamin inhibitors pro-

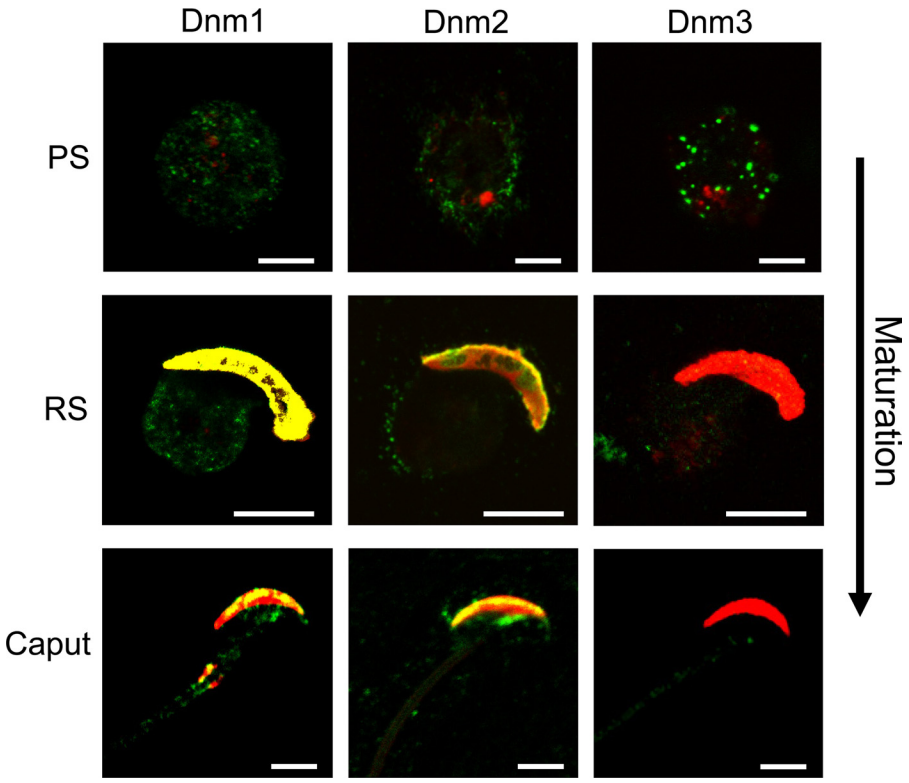

FIGURE 4. **Detection of dynamin isoforms 1–3 in developing mouse spermatozoa.** Enriched populations of sperm cells were collected at various stages of maturation, namely pachytene spermatocytes (*PS*), round spermatids (*RS*), and caput epididymal sperm, and were subjected to immunolabeling with antibodies against dynamin 1, 2, and 3 (*green*). The cells were then counterstained with TRITC-conjugated PNA (*red*), which labels the developing acrosome post-round spermatid stage. As the germ cell matures, dynamin 1 labeling shifted from being ubiquitously distributed throughout the cell to being concentrated in the vicinity of the developing acrosome (colocalized with PNA; *yellow*) within round spermatid and caput spermatozoa. Modest labeling of dynamin 2 was detected on the periphery of pachytene spermatocyte cells before it too became concentrated in the developing acrosome at round spermatid and caput stages. Dynamin 3, however, showed strong punctate labeling in pachytene spermatocyte cells, but as the cells mature this labeling was reduced significantly to the point where it was barely detectable in either round spermatid or caput cells. The images are representative of each germ cell stage. *Scale bars*, 5 μm.

duced a dose-dependent decrease in the levels of progesterone-induced acrosome reaction (Fig. 6*B*). As expected on the basis of its higher potency and cell permeability (26), Dyngo-4a proved a more effective acrosome reaction inhibitor. However, at the highest concentration of each inhibitor, the number of acrosome-reacted spermatozoa was reduced to levels indistinguishable from that of the noncapacitated control sample. These data strongly illustrate that the two stimuli operate via distinct pathways that are dynamin-dependent or dynamin-independent. Because the role of dynamin was linked to progesterone stimulus only, this implies a functional link between dynamin GTPase activity and the ability of spermatozoa to undergo the progesterone-induced acrosome reaction.

Progesterone Challenge Stimulates Phosphorylation of Dynamin 1—The phosphorylation of dynamin 1 and 2 controls their function in an analogous manner. In neurons for instance, dynamin 1 phosphorylation at Ser-778 by Cdk5 and Ser-774 by GSK-3 appears to inhibit its function in activity-dependent bulk endocytosis (27, 44). Although dynamin 2 lacks a serine at the position of Ser-774, it retains a Ser-778-homologous phosphorylation site at Ser-764, which suppresses its function in cytokinesis (45). In view of this mode of regulation, we next examined whether progesterone-induced stimulation of the acrosome reaction involved dynamic regulation of dynamin phosphorylation. Initially, immunoblots were conducted on protein extracted from progesterone-treated mouse spermatozoa to determine the presence of phosphorylated dynamin (Fig. 7). A dominant band was detected for phosphorylated dynamin 1 at both serine 774 (Dnm1p774) and serine 778 (Dnm1p778) at ~100 kDa, confirming the presence of dynamin phosphorylation in progesterone-treated mouse spermatozoa. To examine whether regulation of dynamin phosphorylation was in response to progesterone stimulus, we prepared noncapacitated, capacitated and progesterone treated spermatozoa as well as spermatozoa preincubated with dynasore (100 μM) before stimulation with progesterone. The cells were then immunolabeled for phospho-dynamin 1 (*green*), specifically Ser(P)-774 (Dnm1p774) and Ser(P)-778 (Dnm1p778), and categorized based on the intensity of their periacrosomal labeling. In terms of antibody specificity, it has previously been determined that Dnm1p774 uniquely detects dynamin 1, whereas Dnm1p778 readily detects both dynamin 1 and 2 because the epitopes differ only by a single amino acid (45). Immunolocalization of Dnm1p774 and Dnm1p778 revealed two distinct cellular responses (Fig. 8). For noncapacitated and capacitated samples, the majority of cells were characterized by either weak or absent phospho-dynamin staining in the periacrosomal region of the sperm head, suggestive of low or no constitutive phosphorylation at these sites. Remarkably, stimulation of capacitated cells with progesterone increased the number of

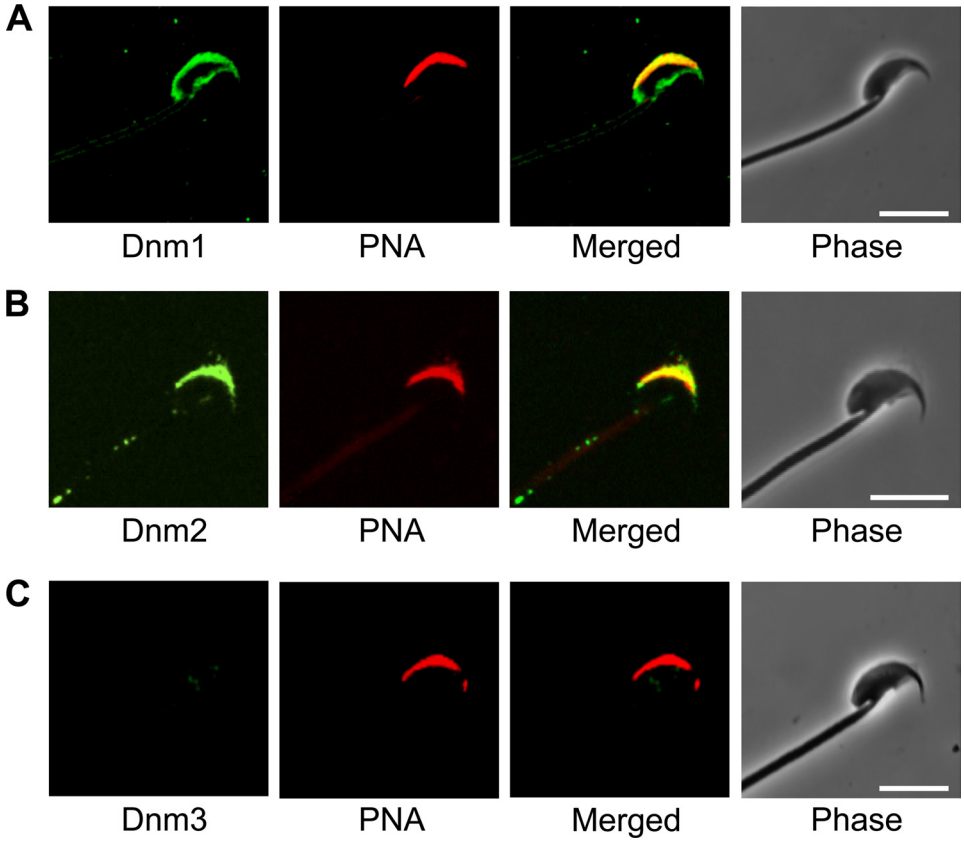

FIGURE 5. **Examination of the localization of dynamin isoforms in mature cauda epididymal spermatozoa.** Antibodies against dynamin isoforms 1, 2, and 3 were used to determine the localization of the three proteins (*green*), and these cells were then counterstained with the TRITC-conjugated (*red*) acrosomal marker, PNA. Both dynamin isoforms 1 and 2 (*A* and *B*, respectively; *green*) were strongly colocalized with PNA within the acrosomal region. In contrast, dynamin 3 (*C*) was not able to be detected in these cells. Representative images are shown. *Scale bars*, 10 μm.

spermatozoa exhibiting intense Dnm1p774 and Dnm1p778 labeling within this region of the head (Fig. 8, *C* and *G*, *arrow*). Surprisingly, incubation of sperm in capacitation permissive medium supplemented with dynasore abolished this apparent increase in phosphorylation (Fig. 8, *D* and *H*).

To determine whether these phosphorylation events were regulated via Ca^{2+} mobilization upon progesterone treatment, we repeated the experiment in the presence of the intracellular Ca^{2+} chelator, BAPTA-AM (10 μM). Following brief incubation of spermatozoa in BAPTA-AM, progesterone challenge failed to elicit increased dynamin phosphorylation at either of the phosphorylation target sites (Fig. 8*J*).

Effects of Dynamin Inhibitors on Fertilization Potential—In view of the evidence that *in vitro* pharmacological inhibition of dynamin 1 and 2 elicits a potent reduction in the number of acrosome reaction events in progesterone-treated spermatozoa, we next aimed to determine whether these effects could abrogate fertilization *in vitro*. To address this question, mouse spermatozoa were capacitated in the presence of the dynamin inhibitors Dyngo-4a (10 μM) and dynasore (10 μM) and subsequently added to oocytes recovered from super ovulated females *in vitro*. Assessment of fertility was made by counting the number of two-cell embryos present after overnight incubation with both dynamin-inhibited and control spermatozoa (Fig. 9*A*). The results of this study revealed a significant reduction in the number of two-cell embryos present and thus a reduction in the fertilization rate within the dynamin-inhibited populations. These data indicate that dynamin activity is required for fertilization to occur *in vitro*. Such a result strengthens the argument that dynamin fulfills an important role during fertilization through its ability to regulate the acrosome reaction.

Finally, because we had demonstrated that an inhibition of dynamin *in vitro* led to suppression of acrosome reactions under progesterone stimulus, we investigated whether these results could be reproduced following *in vivo* administration of the dynamin inhibitors. For this purpose, adult male mice were injected with dynamin inhibitors at a concentration previously found to inhibit dynamin in neurons. After 5 days, their spermatozoa were isolated and assessed for their ability to acrosome react *in vitro*. Interestingly, despite no overt changes in either motility or viability, the *in vivo* administration of either Dyngo-4a or dynasore did appear to significantly suppress the ability of sperm to undergo acrosomal exocytosis in response to progesterone challenge (Fig. 9*B*). In contrast, normal rates of acrosome reaction were recorded in sperm recovered from males treated with the vehicle (Me_2SO) control. Such findings highlight the potential of targeting dynamin as a means of fertility regulation.

DISCUSSION

The large GTPase dynamin is well known for its roles during vesicle trafficking with the majority of mammalian studies focusing on dynamin regulation of neural pathways (46–48).

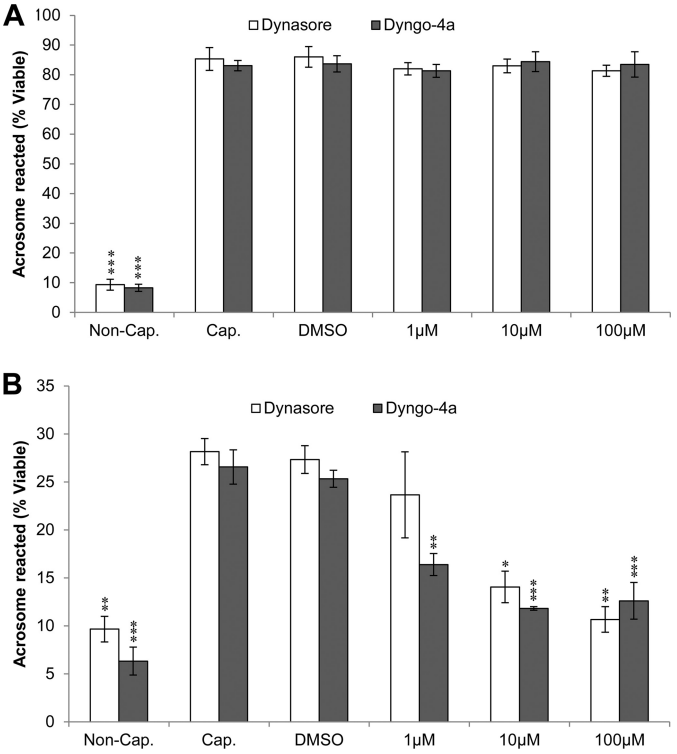

FIGURE 6. **Investigation of the effect of pharmacological inhibition of dynamin on the ability of mouse spermatozoa to engage in acrosomal exocytosis.** Mouse spermatozoa were either noncapacitated (*Non-Cap.*), capacitated (*Cap.*), or capacitated in the presence of two different inhibitors of dynamin 1 and 2 (dynasore and Dyngo-4a). Each inhibitor was used at three different concentrations, namely 1, 10, and 100 μM. Viable cells were recorded as acrosome reacted upon the loss of PNA staining when viewed by fluorescence microscopy. *A*, there was no reduction in the number of acrosome-reacted cells at any concentration of inhibitor in the 2.5 μM A23187-induced treatments when compared with Me_2SO vehicle control (*DMSO*). *B*, there was, however, a significant ($P < 0.05$) reduction in the number of acrosome-reacted cells for all treatments at medium and high inhibitor concentrations when the progesterone-induced (15 μM) acrosome reaction was assayed. Each experiment was replicated three times, and the results are presented as the means ± S.E. *, $P < 0.05$; **, $P < 0.01$; ***, $P < 0.001$.

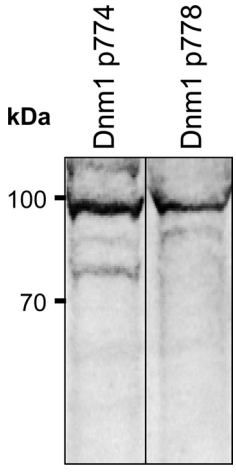

FIGURE 7. **Identification of Dnm1p774 and Dnm1p778 in protein extracted from progesterone-treated (15 μM) mouse spermatozoa.** SDS extracted protein from progesterone treated mouse spermatozoa (40 μg) was separated via SDS-PAGE followed by transfer onto nitrocellulose membranes and labeling with antibodies directed against dynamin 1 p774 and dynamin 1 p778. A dominant band at ~100 kDa indicates that both phosphorylated versions were detected in progesterone-treated mouse spermatozoa. These experiments were repeated three times using pooled semen samples from at least three mice, and representative immunoblots are shown.

There is also significant interest in studying dynamin from a reproductive standpoint because vesicle trafficking plays major roles in producing functional spermatozoa. During spermatogenesis, the vesicle-mediated formation of the acrosome is an integral step in producing spermatozoa with the ability to fertilize the egg (44, 49), although the realization of this ability, namely the acrosome reaction, is based on the regulated formation of membrane vesicles and therefore requires the interplay of membrane vesicle manipulators (12, 13). Here we report the spatial and temporal expression of the three classical dynamin proteins in maturing (post-spermatogonial) male germ cells and for the first time demonstrate that both dynamin 1 and 2 are retained within fully mature mouse spermatozoa. We have established that dynamin 1 and/or 2 undergoes changes in phosphorylation pattern within fully mature spermatozoa in response to exposure to the steroid hormone progesterone. Furthermore we have provided the first evidence that pharmacological inhibition of dynamin 1 and 2 leads to a significant reduction in the number of spermatozoa that are competent to undergo the progesterone-induced acrosome reaction both *in vitro* and *in vivo*.

Association of dynamin 2 with Golgi-derived vesicles has been well documented in various somatic cell types, in which it is necessary for the formation of newly budded vesicles (50–53), and appears to be a regulator of post-Golgi vesicle exocytosis at the plasma membrane (3). During spermatogenesis, structures analogous to these Golgi-derived vesicles known as pro-acrosomal vesicles fuse, not at the plasma membrane, but along an internal structure called the acroplaxome to form the acrosome (49, 54). Localization of dynamin 1 and 2 to the crescent structure observed in testis sections is indicative of the proteins being expressed in the surrounding membrane of the enlarging spherical acrosome. Indeed as the spherical acrosomic granule increases in size and changes in shape throughout the Golgi and cap phases of spermiogenesis, respectively, vesicle transport and fusion machinery are highly active (55–57). The pattern of localization for dynamin suggests a role for the large GTPase in regulating these multiple fusion events occurring across the entirety of the developing acrosome and is supported by the shift in the dynamin localization pattern as germ cell maturation proceeds (Fig. 2, *B–D* and *F–H*). Interestingly, two proteins that mimic the staining pattern of dynamin 1 and 2 throughout mouse germ cell maturation are ZPBP1 and ZPBP2 (zona pellucida binding proteins 1 and 2) (58). In addition to their potential roles during sperm-zona interactions (59), these two proteins have been found to be necessary for correct formation of the mouse sperm acrosome (58). The remarkably similar localization patterns to those of the zona pellucida binding proteins places dynamins 1 and 2 in a position that is compatible with a key role in the regulation of acrosome biogenesis.

The overlapping patterns of dynamin 1 and 2 localization contrast with that of dynamin 3, which was found to be exclusively expressed within a series of discrete, punctate patches. This punctate localization may reflect regions of vesicle transport, or alternatively, they may correspond to locations in which the germ cell attaches to the Sertoli cell. An example of this form of attachment is the tubulobulbar complex, the for-

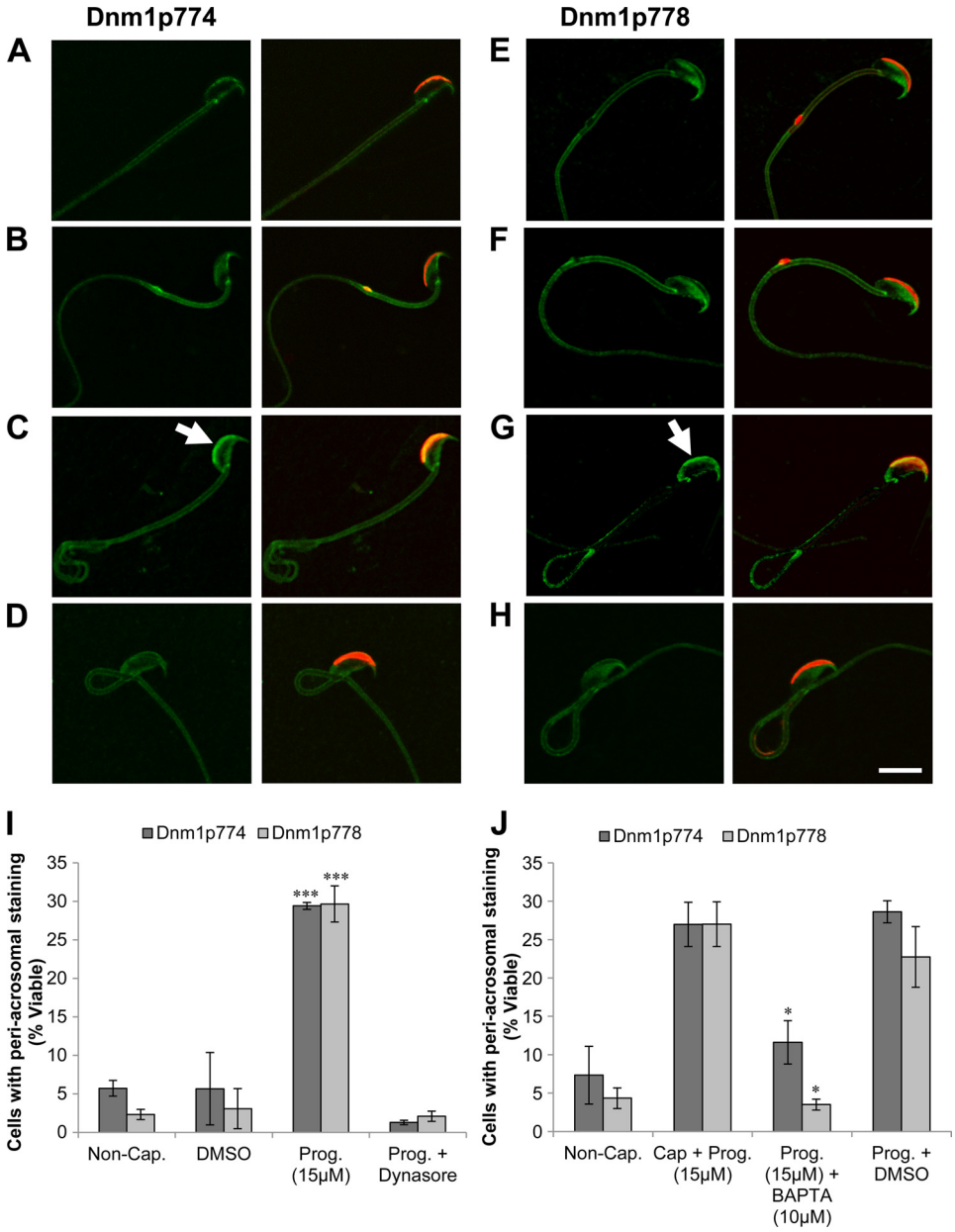

FIGURE 8. **Progesterone treatment leads to an increase in cells exhibiting Dnm1p774 and Dnm1p778 labeling which can be prevented via preincubation with dynasore.** Immunolabeling of Dnm1p774/Dnm1p778 (*green*) with the periacrosomal marker PNA (*red*) was conducted in the following populations of spermatozoa: noncapacitated (*Non-Cap.*) (*A* and *E*); capacitated + Me_2SO (*DMSO*) (*B* and *F*); capacitated + progesterone (*Prog.*) (*C* and *G*); and capacitated + dynasore + progesterone (*Prog. + Dynasore*) (*D* and *H*). Cells exhibiting intense periacrosomal labeling for Dnm1p774/Dnm1p778 were quantified (*I*). These data revealed that progesterone challenge elicited a highly significant increase in Dnm1p774/Dnm1p778 staining compared with Me_2SO control and that this staining could be prevented by incubation of the cells with dynasore during their capacitation. Similarly, incubating the cells with the Ca^{2+} chelator, BAPTA-AM, prior to progesterone treatment (*J*) also resulted in a significant reduction in Dnm1 phosphorylation. Representative images shown for each treatment. Each experiment was replicated three times, and the results are presented as the means ± S.E. *, $p < 0.05$; ***, $p < 0.001$.

mation of which has been shown to involve dynamin 3 and potentially dynamin 2 (7, 60–62). Indeed, dynamin 3 appears to determine the morphology of the multiple tubulobulbar complexes that exist per germ cell and possibly promotes formation of large double membrane vesicles from these complexes (7). Irrespective of its role in the testes, the fact that dynamin 3 is lost prior to the release of spermatozoa from the testes argues against the protein having a direct role in fertilization.

Our study is the first to report the retention of both dynamin 1 and 2 from germ cells of the mammalian testes through to fully mature spermatozoa. The presence of these proteins in developing germ cells indicates likely roles in vesicle endo/exocytosis that may be required for intercellular signaling between these cells and the supporting Sertoli cells (63, 64). Indeed less intense, nonacrosomal labeling for dynamin 1 and 2 around the periphery of a number of maturing germ cells (Fig. 2, *A* and *E*, *arrowheads*) appears to confirm the presence of these germ cell/Sertoli cell signaling gateways. Signaling events involving dynamin have been related to dynamic changes in the blood-testis barrier (65, 66), although our immunofluorescence studies were unable to localize dynamin to this region. Because

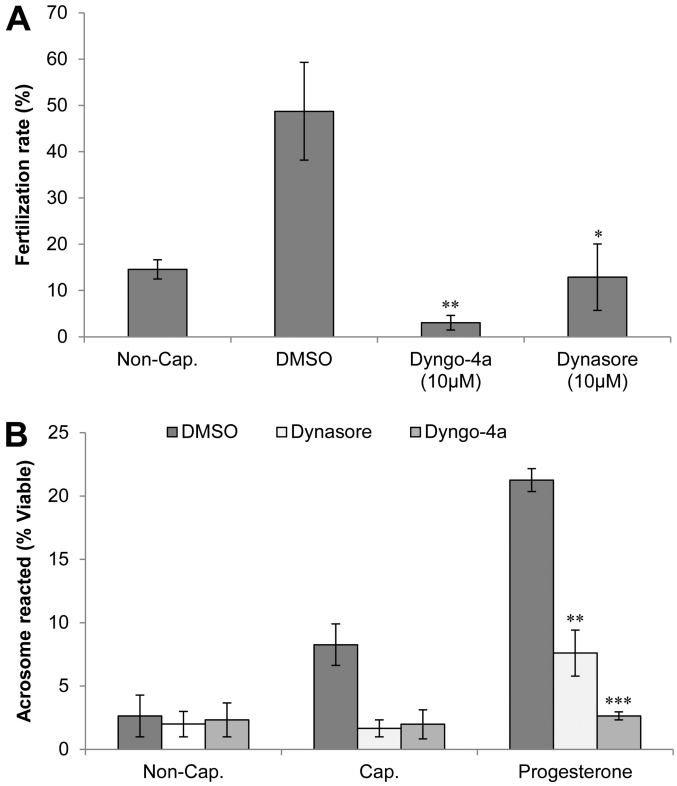

FIGURE 9. *A*, effect of dynamin inhibitors on *in vitro* fertilization. Spermatozoa from male mice were prepared into populations of noncapacitated (*Non-Cap.*), capacitated (*Cap.*), Dyngo-4a-treated (10 μM), or dynasore-treated (10 μM) and were subsequently introduced into medium containing mouse oocytes. Following incubation, the fertilization rate was determined by counting two-cell embryos and expressing this as a percentage of total oocytes/treatment. These data demonstrate a significant reduction in the fertilization rate of dynamin-inhibited samples compared with the Me_2SO vehicle control (*DMSO*). *B*, investigation into the effect of pharmacological inhibition of dynamin 1 and 2 *in vivo*. Male mice were injected intraperitoneally twice with either Dyngo-4a (1.5 mg), Dynasore (1.5 mg), or Me_2SO (control, *DMSO*). Following recovery of the spermatozoa from injected males, populations of noncapacitated (*Non-Cap.*) and capacitated (*Cap.*) cells were prepared. The latter were challenged with progesterone (15 μM) to induce acrosomal exocytosis. Viable cells from each treatment group were recorded as acrosome reacted upon the loss of PNA staining when viewed by fluorescence microscopy. These data demonstrate the expected increase in acrosome reaction numbers in spermatozoa from the Me_2SO control males, whereas a significant reduction was seen in both dynamin-inhibited treatments. Each experiment was replicated three times, and the results are presented as the means ± S.E. *, $P < 0.05$; **, $P < 0.01$; ***, $P < 0.001$.

these studies were performed in rat, this may reflect species-specific differences in the function of dynamin, inaccessibility of target antigens, and/or be a result of different antibodies being utilized. Previous studies have implicated dynamin 2 in essential roles within the mammalian testis, such as internalization and degradation of the connexin 43 gap junction plaques within the blood-testis barrier (67), and phosphatidylserine-dependent phagocytosis of residual bodies via both actin assembly as well as through interactions with amphiphysin 1 (68, 69). It is therefore becoming more apparent that dynamin contributes to the process of spermatogenesis through the regulation of a number of events that rely upon vesicle trafficking.

Importantly, our data highlight a potentially novel function for this large GTPase, post-spermatogenesis. The changes in dynamin localization that occur during germ cell differentiation demonstrate that these proteins are clearly retained within the acrosomal region of morphologically mature spermatozoa (Fig. 5). Such findings raise questions regarding whether this localization is simply a remnant of the proteins previous role in acrosome formation or whether they may be of further functional significance to the cell during acrosomal exocytosis. Utilizing the dynamin inhibitors dynasore and Dyngo-4a, we have demonstrated that dynamin does have a functional role in mature spermatozoa and that this function is intimately linked to the induction of a progesterone driven acrosome reaction. Indeed, pharmacological inhibition of dynamin 1 and 2 potently reduced the ability of spermatozoa to respond to the stimulus of progesterone challenge by undergoing acrosomal exocytosis. Remarkably, this inhibitory effect extended to the spermatozoa of mice treated with an acute dose of the relevant inhibitors. Furthermore, we have demonstrated that dynamin inhibition causes a significant reduction in fertilization potential of spermatozoa in *in vitro* fertilization studies. Taken together, these data encourage further analysis of dynamin as a potential target for fertility regulation.

Notwithstanding the ability of dynamin inhibitors to suppress a progesterone-induced acrosome reaction, an equivalent reduction was not seen when stimulation was induced via the calcium ionophore, A23187. The key difference between a progesterone- and A23187-induced acrosome reaction is that the latter effectively bypasses the key regulatory mechanisms normally required to facilitate induction of this exocytotic event. In contrast, evidence suggests that exposure of capacitated mouse spermatozoa to progesterone leads to stimulation of ion channels hypothesized to regulate downstream signaling and ultimately the key proteins/molecules involved in acrosomal exocytosis. One such intermediary that may be directly responsible for dynamin regulation is phospholipase C (PLC) (specifically PLCδ4 in mouse). This enzyme is central to phosphoinositide metabolism because of its ability to hydrolyze phosphatidylinositol 4,5-bisphosphate into the second messengers inositol 1,4,5-trisphosphate and diacylglycerol. These second messengers are, in turn, important for intercellular signaling and membrane trafficking (43, 70). It has also been shown that progesterone can activate PLA_2 in spermatozoa via the stimulation of a G-protein pathway (71). In other cell types, PLA_2 and dynamins 1 and 2 are required to promote cholesterol-induced Golgi vesiculation, an event that is analogous to that of acrosomal exocytosis (53), although the mechanism by which PLA_2 and dynamin act has not yet been well defined.

We have also demonstrated that challenging capacitating spermatozoa with progesterone is capable of stimulating the phosphorylation of dynamin 1 on serine residues 774 and 778. However, this effect was entirely ablated by prior incubation of sperm with either dynasore (100 μM) or the Ca^{2+} chelator, BAPTA-AM (Fig. 8). Importantly, phosphorylation of dynamin 1 on these specific residues in neural cells has been found to down-regulate its GTPase activity and promote a relocation of the protein from membrane to cytosol (72). Interestingly, a reduction in dynamin GTPase activity has recently been shown to promote the stabilization of exocytotic post fusion pores and thereby influence the rate of fusion pore expansion during exocytosis (73). Such modifications may therefore account for the unique, slower form of exocytosis observed during the acro-

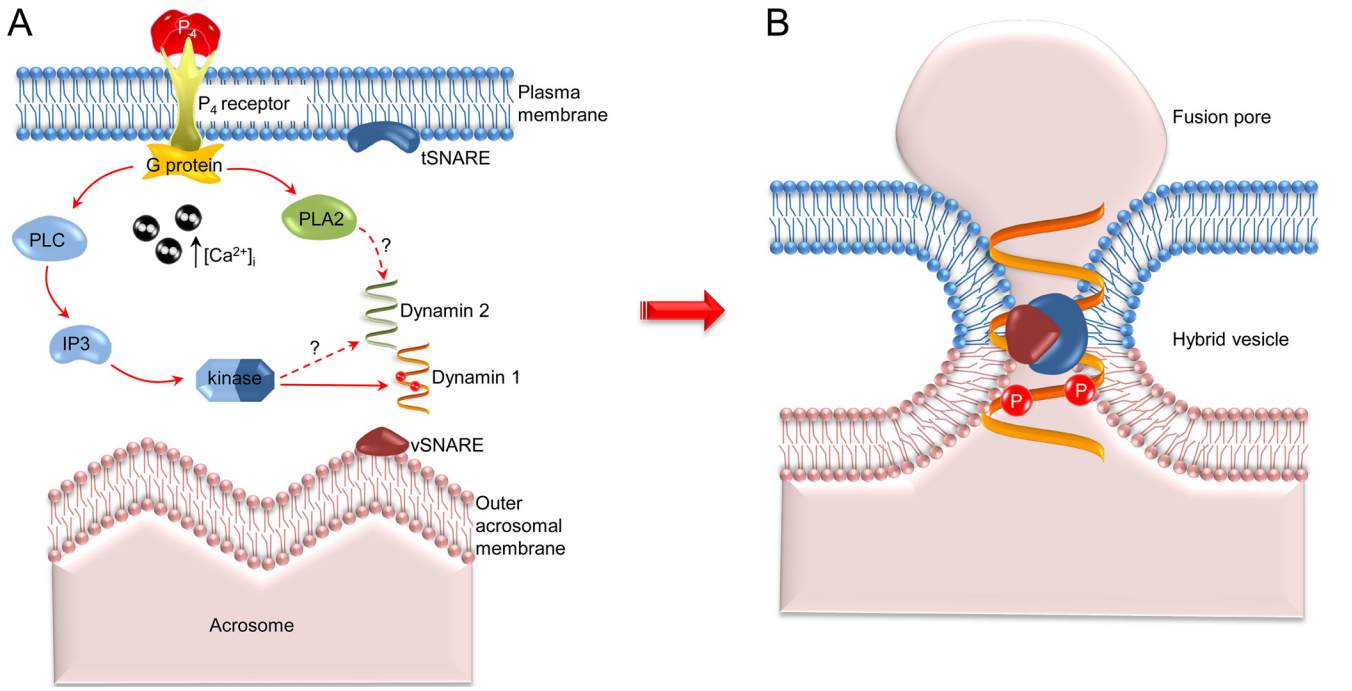

FIGURE 10. **Model of dynamin mechanism of action during the progesterone induced acrosome reaction in mouse spermatozoa.** *A*, on the basis of previous studies, it is proposed that progesterone challenge stimulates receptors in the plasma membrane, leading to an increase in $[Ca^{2+}]_i$ and activation of a G-protein-mediated signal transduction cascade incorporating PLC and PLA_2, both of which are required for the acrosome reaction (71). PLC stimulates production of inositol 1,4,5-trisphosphate (IP3) and eventually results in the downstream activation of an intermediary kinase that phosphorylates dynamin on serine residues 774 and 778. These changes coincide with the assembly of SNARE proteins, altering their resting *cis*-configuration into an active *trans*-configuration that is capable of mediating the fusion of the outer acrosomal and plasma membranes (20). *B*, we propose that dynamin may indirectly associate with the SNARE protein complex at regions of membrane fusion via their interactions with complexins (8). Upon phosphorylation of serines 774 and 778 and a corresponding reduction in their GTPase activity, dynamin would then be positioned to stabilize the newly formed fusion pores and/or slow fusion pore expansion rate, thus leading to the prolonged exocytotic event that characterizes the sperm acrosome reaction.

some reaction. In neural cells, the phosphorylation of dynamin 1 on serines 774/778 is driven by cyclin-dependent kinase 5 (cdk5) (27, 74) and Ser-774 by GSK3 (44), whereas in HeLa cells CDK2 phosphorylates dynamin 2 at Ser-764 (the orthologous site to Ser-778) (75); however, it remains to be established whether equivalent enzymes are present in mouse spermatozoa and what signals may regulate their activity.

Another important function of dynamin is that of synaptic vesicle recycling, in which dynamin localizes to, and assembles around, newly formed fusion necks. Through its fission action, dynamin is able to prevent vesicle collapse into the target membrane, and thus vesicle and plasma membranes remain separate (76). The mechanisms that underpin the association of dynamin with these newly formed fusion pores remains unresolved; however, a link between dynamin and the fusion-competent SNARE proteins could potentially arise through association with complexins I and II, previously established within mouse spermatozoa (8). As spermatozoa progress through capacitation, evidence suggests that their outer acrosomal membrane becomes ruffled and, as a consequence, comes into close proximity with the plasma membrane (77). We anticipate that the proximity of these membranes would increase the likelihood of spontaneous fusion events occurring and therefore would result in the localization of dynamin to these areas. Importantly, inhibition of dynamin during capacitation would perturb the ability of the enzyme to associate with proteins necessary for regulating fusion and thus be unable to fulfill its role in fusion pore stabilization. In this study we have shown that inhibition with dynasore prevents phosphorylation of dynamin 1 on serines 774 and 778. This result was unexpected but could arise from nonspecific, steric hindrance of the target phosphorylation sites. In this regard dynasore is known to interfere with the GTPase domain of dynamin, a region that lies proximal to these C-terminal residues (78). Although we cannot determine whether dynamin 2 is also phosphorylated from these data, it is curious that both isoforms were detected within overlapping domains in mature spermatozoa. This finding raises the prospect of functional redundancy, with dynamin 1 and 2 cooperating in supporting optimal rates of acrosomal exocytosis. This notion is consistent with previous studies that have highlighted the ability of different dynamin isoforms to exert similar roles in somatic cells (79, 80).

On the basis of our collective data, we propose a model (Fig. 10) in which the post-translational modifications of dynamin that occur in response to progesterone-induced Ca^{2+} influx, act to regulate the role of the enzyme in controlling fusion pore dynamics and thereby deliver one of the slowest exocytotic events in nature (81). Testing this novel model promises to shed light on what continues to be a critical yet highly elusive process.

REFERENCES

1. Shpetner, H. S., and Vallee, R. B. (1989) Identification of dynamin, a novel mechanochemical enzyme that mediates interactions between microtu-

bules. *Cell* **59,** 421–432
2. Hinshaw, J. E., and Schmid, S. L. (1995) Dynamin self-assembles into rings suggesting a mechanism for coated vesicle budding. *Nature* **374,** 190–192
3. Jaiswal, J. K., Rivera, V. M., and Simon, S. M. (2009) Exocytosis of post-Golgi vesicles is regulated by components of the endocytic machinery. *Cell* **137,** 1308–1319
4. Cao, H., Thompson, H. M., Krueger, E. W., and McNiven, M. A. (2000) Disruption of Golgi structure and function in mammalian cells expressing a mutant dynamin. *J. Cell Sci.* **113,** 1993–2002
5. Sontag, J. M., Fykse, E. M., Ushkaryov, Y., Liu, J. P., Robinson, P. J., and Südhof, T. C. (1994) Differential expression and regulation of multiple dynamins. *J. Biol. Chem.* **269,** 4547–4554
6. Cao, H., Garcia, F., and McNiven, M. A. (1998) Differential distribution of dynamin isoforms in mammalian cells. *Mol. Biol. Cell* **9,** 2595–2609
7. Vaid, K. S., Guttman, J. A., Babyak, N., Deng, W., McNiven, M. A., Mochizuki, N., Finlay, B. B., and Vogl, A. W. (2007) The role of dynamin 3 in the testis. *J. Cell Physiol.* **210,** 644–654
8. Zhao, L., Shi, X., Li, L., and Miller, D. J. (2007) Dynamin 2 associates with complexins and is found in the acrosomal region of mammalian sperm. *Mol. Reprod. Dev.* **74,** 750–757
9. McMahon, H. T., Missler, M., Li, C., and Südhof, T. C. (1995) Complexins. Cytosolic proteins that regulate SNAP receptor function. *Cell* **83,** 111–119
10. Jin, M., Fujiwara, E., Kakiuchi, Y., Okabe, M., Satouh, Y., Baba, S. A., Chiba, K., and Hirohashi, N. (2011) Most fertilizing mouse spermatozoa begin their acrosome reaction before contact with the zona pellucida during in vitro fertilization. *Proc. Natl. Acad. Sci.* **108,** 4892–4896
11. Liu, D. Y., and Baker, H. W. (2003) Disordered zona pellucida-induced acrosome reaction and failure of in vitro fertilization in patients with unexplained infertility. *Fertil. Steril.* **79,** 74–80
12. Barros, C., Bedford, J. M., Franklin, L. E., and Austin, C. R. (1967) Membrane vesiculation as a feature of the mammalian acrosome reaction. *J. Cell Biol.* **34,** C1–C5
13. Yanagimachi, R., and Noda, Y. D. (1970) Electron microscope studies of sperm incorporation into the golden hamster egg. *Am. J. Anat.* **128,** 429–462
14. Austin, C. R. (1951) Observations on the penetration of the sperm in the mammalian egg. *Aust. J. Sci. Res. B* **4,** 581–596
15. Chang, M. C. (1951) Fertilizing capacity of spermatozoa deposited into the fallopian tubes. *Nature* **168,** 697–698
16. Visconti, P. E., Bailey, J. L., Moore, G. D., Pan, D., Olds-Clarke, P., and Kopf, G. S. (1995) Capacitation of mouse spermatozoa. I. Correlation between the capacitation state and protein tyrosine phosphorylation. *Development* **121,** 1129–1137
17. Reid, A. T., Redgrove, K., Aitken, R. J., and Nixon, B. (2011) Cellular mechanisms regulating sperm. Zona pellucida interaction. *Asian J. Androl.* **13,** 88–96
18. Arnoult, C., Cardullo, R. A., Lemos, J. R., and Florman, H. M. (1996) Activation of mouse sperm T-type Ca^{2+} channels by adhesion to the egg zona pellucida. *Proc. Natl. Acad. Sci. U.S.A.* **93,** 13004–13009
19. Jungnickel, M. K., Marrero, H., Birnbaumer, L., Lémos, J. R., and Florman, H. M. (2001) Trp2 regulates entry of Ca^{2+} into mouse sperm triggered by egg ZP3. *Nat. Cell Biol.* **3,** 499–502
20. De Blas, G. A., Roggero, C. M., Tomes, C. N., and Mayorga, L. S. (2005) Dynamics of SNARE assembly and disassembly during sperm acrosomal exocytosis. *PLoS Biol.* **3,** e323
21. Daly, C., and Ziff, E. B. (2002) Ca^{2+}-dependent formation of a dynamin-synaptophysin complex. *J. Biol. Chem.* **277,** 9010–9015
22. Gorini, G., Ponomareva, O., Shores, K. S., Person, M. D., Harris, R. A., and Mayfield, R. D. (2010) Dynamin-1 co-associates with native mouse brain BKCa channels. Proteomics analysis of synaptic protein complexes. *FEBS Lett.* **584,** 845–851
23. Peters, C., Baars, T. L., Bühler, S., and Mayer, A. (2004) Mutual control of membrane fission and fusion proteins. *Cell* **119,** 667–678
24. Bürmann, F., Ebert, N., van Baarle, S., and Bramkamp, M. (2011) A bacterial dynamin-like protein mediating nucleotide-independent membrane fusion. *Mol. Microbiol.* **79,** 1294–1304
25. Miyauchi, K., Kim, Y., Latinovic, O., Morozov, V., and Melikyan, G. B. (2009) HIV enters cells via endocytosis and dynamin-dependent fusion with endosomes. *Cell* **137,** 433–444
26. Harper, C. B., Martin, S., Nguyen, T. H., Daniels, S. J., Lavidis, N. A., Popoff, M. R., Hadzic, G., Mariana, A., Chau, N., McCluskey, A., Robinson, P. J., and Meunier, F. A. (2011) Dynamin inhibition blocks botulinum neurotoxin type A endocytosis in neurons and delays botulism. *J. Biol. Chem.* **286,** 35966–35976
27. Tan, T. C., Valova, V. A., Malladi, C. S., Graham, M. E., Berven, L. A., Jupp, O. J., Hansra, G., McClure, S. J., Sarcevic, B., Boadle, R. A., Larsen, M. R., Cousin, M. A., and Robinson, P. J. (2003) Cdk5 is essential for synaptic vesicle endocytosis. *Nat. Cell Biol.* **5,** 701–710
28. Enders, G. C., and May, J. J., 2nd (1994) Developmentally regulated expression of a mouse germ cell nuclear antigen examined from embryonic day 11 to adult in male and female mice. *Dev. Biol.* **163,** 331–340
29. Odell, L. R., Chau, N., Mariana, A., Graham, M. E., Robinson, P. J., and McCluskey, A. (2009) Azido and diazarinyl analogues of bis-tyrphostin as asymmetrical inhibitors of dynamin gTPase. *ChemMedChem* **4,** 1182–1188
30. Hill, T. A., Mariana, A., Gordon, C. P., Odell, L. R., Robertson, M. J., McGeachie, A. B., Chau, N., Daniel, J. A., Gorgani, N. N., Robinson, P. J., and McCluskey, A. (2010) Iminochromene inhibitors of dynamins I and II GTPase activity and endocytosis. *J. Med. Chem.* **53,** 4094–4102
31. Nixon, B., Bielanowicz, A., McLaughlin, E. A., Tanphaichitr, N., Ensslin, M. A., and Aitken, R. J. (2009) Composition and significance of detergent resistant membranes in mouse spermatozoa. *J. Cell Physiol.* **218,** 122–134
32. Asquith, K. L., Baleato, R. M., McLaughlin, E. A., Nixon, B., and Aitken, R. J. (2004) Tyrosine phosphorylation activates surface chaperones facilitating sperm-zona recognition. *J. Cell Sci.* **117,** 3645–3657
33. Nixon, B., MacIntyre, D. A., Mitchell, L. A., Gibbs, G. M., O'Bryan, M., and Aitken, R. J. (2006) The identification of mouse sperm-surface-associated proteins and characterization of their ability to act as decapacitation factors. *Biol. Reprod.* **74,** 275–287
34. Biggers, J. D., Whitten, W. K., and Whittingham, D. G. (1971) The culture of mouse embryos *in vitro*, in *Methods in Mammalian Embryology* (Daniel, J. C. ed.) pp. 86–116, Freeman Press, San Francisco, CA
35. Baleato, R. M., Aitken, R. J., and Roman, S. D. (2005) Vitamin A regulation of BMP4 expression in the male germ line. *Dev. Biol.* **286,** 78–90
36. Russell, L. D., Ettlin, R., Sinha Hikim, A., and Clegg, E. (1990) *Histological and Histopathological Evaluation of the Testis*, Cache River Press, Clearwater, FL
37. Aitken, R. J., Buckingham, D. W., and Fang, H. G. (1993) Analysis of the responses of human spermatozoa to A23187 employing a novel technique for assessing the acrosome reaction. *J. Androl.* **14,** 132–141
38. Takeo, T., and Nakagata, N. (2011) Reduced glutathione enhances fertility of frozen/thawed C57BL/6 mouse sperm after exposure to methyl-β-cyclodextrin. *Biol. Reprod.* **85,** 1066–1072
39. Quinn, P., Kerin, J. F., and Warnes, G. M. (1985) Improved pregnancy rate in human *in vitro* fertilization with the use of a medium based on the composition of human tubal fluid. *Fertil. Steril.* **44,** 493–498
40. Viggiano, J. M., Herrero, M. B., Martínez, S. P., and De Gimeno, M. F. (1996) Analysis of the effect of nitric oxide synthase inhibition on mouse sperm employing a modified staining method for assessment of the acrosome reaction. *J. Androl.* **17,** 692–698
41. Moreno, R. D., Ramalho-Santos, J., Sutovsky, P., Chan, E. K., and Schatten, G. (2000) Vesicular traffic and Golgi apparatus dynamics during mammalian spermatogenesis. Implications for acrosome architecture. *Biol. Reprod.* **63,** 89–98
42. Macia, E., Ehrlich, M., Massol, R., Boucrot, E., Brunner, C., and Kirchhausen, T. (2006) Dynasore, a cell-permeable Inhibitor of dynamin. *Dev. Cell* **10,** 839–850
43. Roldan, E. R., Murase, T., and Shi, Q. X. (1994) Exocytosis in spermatozoa in response to progesterone and zona pellucida. *Science* **266,** 1578–1581
44. Clayton, E. L., Sue, N., Smillie, K. J., O'Leary, T., Bache, N., Cheung, G., Cole, A. R., Wyllie, D. J., Sutherland, C., Robinson, P. J., and Cousin, M. A. (2010) Dynamin I phosphorylation by GSK3 controls activity-dependent bulk endocytosis of synaptic vesicles. *Nat. Neurosci.* **13,** 845–851
45. Chircop, M., Sarcevic, B., Larsen, M. R., Malladi, C. S., Chau, N., Zavortink, M., Smith, C. M., Quan, A., Anggono, V., Hains, P. G., Graham, M. E.,

and Robinson, P. J. (2011) Phosphorylation of dynamin II at serine-764 is associated with cytokinesis. *Biochim. Biophys. Acta* **1813,** 1689–1699
46. Robinson, P. J., Sontag, J. M., Liu, J. P., Fykse, E. M., Slaughter, C., McMahon, H., and Südhof, T. C. (1993) Dynamin GTPase regulated by protein kinase C phosphorylation in nerve terminals. *Nature* **365,** 163–166
47. Takei, K., McPherson, P. S., Schmid, S. L., and De Camilli, P. (1995) Tubular membrane invaginations coated by dynamin rings are induced by GTP-γS in nerve terminals. *Nature* **374,** 186–190
48. Raimondi, A., Ferguson, S. M., Lou, X., Armbruster, M., Paradise, S., Giovedi, S., Messa, M., Kono, N., Takasaki, J., Cappello, V., O'Toole, E., Ryan, T. A., and De Camilli, P. (2011) Overlapping role of dynamin isoforms in synaptic vesicle endocytosis. *Neuron* **70,** 1100–1114
49. Fawcett, D. W., and Hollenberg, R. D. (1963) Changes in the acrosome of guinea pig spermatozoa during passage through the epididymis. *Z Zellforsch Mikrosk Anat.* **60,** 276–292
50. Kreitzer, G., Marmorstein, A., Okamoto, P., Vallee, R., and Rodriguez-Boulan, E. (2000) Kinesin and dynamin are required for post-Golgi transport of a plasma-membrane protein. *Nat. Cell Biol.* **2,** 125–127
51. Jones, S. M., Howell, K. E., Henley, J. R., Cao, H., and McNiven, M. A. (1998) Role of dynamin in the formation of transport vesicles from the trans-Golgi network. *Science* **279,** 573–577
52. Kessels, M. M., Dong, J., Leibig, W., Westermann, P., and Qualmann, B. (2006) Complexes of syndapin II with dynamin II promote vesicle formation at the trans-Golgi network. *J. Cell Sci.* **119,** 1504–1516
53. Grimmer, S., Ying, M., Wälchli, S., van Deurs, B., and Sandvig, K. (2005) Golgi vesiculation induced by cholesterol occurs by a dynamin- and cPLA2-dependent mechanism. *Traffic* **6,** 144–156
54. Kierszenbaum, A. L., Rivkin, E., and Tres, L. L. (2003) Acroplaxome, an F-actin-keratin-containing plate, anchors the acrosome to the nucleus during shaping of the spermatid head. *Mol. Biol. Cell* **14,** 4628–4640
55. Abou-Haila, A., and Tulsiani, D. R. (2000) Mammalian sperm acrosome. Formation, contents, and function. *Arch. Biochem. Biophys.* **379,** 173–182
56. Leblond, C. P., and Clermont, Y. (1952) Definition of the stages of the cycle of the seminiferous epithelium in the rat. *Ann. N.Y. Acad. Sci.* **55,** 548–573
57. Kang-Decker, N., Mantchev, G. T., Juneja, S. C., McNiven, M. A., and van Deursen, J. M. (2001) Lack of acrosome formation in Hrb-deficient mice. *Science* **294,** 1531–1533
58. Lin, Y. N., Roy, A., Yan, W., Burns, K. H., and Matzuk, M. M. (2007) Loss of zona pellucida binding proteins in the acrosomal matrix disrupts acrosome biogenesis and sperm morphogenesis. *Mol. Cell Biol.* **27,** 6794–6805
59. Buffone, M. G., Foster, J. A., and Gerton, G. L. (2008) The role of the acrosomal matrix in fertilization. *Int. J. Dev. Biol.* **52,** 511–522
60. Guttman, J. A., Takai, Y., and Vogl, A. W. (2004) Evidence that tubulobulbar complexes in the seminiferous epithelium are involved with internalization of adhesion junctions. *Biol. Reprod.* **71,** 548–549
61. Cheng, C. Y., Vogl, A. W., Vaid, K. S., and Guttman, J. A. (2009) The Sertoli cell cytoskeleton, in *Molecular Mechanisms in Spermatogenesis*, pp. 186–211, Springer, New York
62. Kusumi, N., Watanabe, M., Yamada, H., Li, S. A., Kashiwakura, Y., Matsukawa, T., Nagai, A., Nasu, Y., Kumon, H., and Takei, K. (2007) Implication of amphiphysin 1 and dynamin 2 in tubulobulbar complex formation and spermatid release. *Cell Struct. Funct.* **32,** 101–113
63. Djakiew, D., and Dym, M. (1988) Pachytene spermatocyte proteins influence sertoli cell function. *Biol. Reprod.* **39,** 1193–1205
64. Page, K. C., Mason, P. B., Lindstrom, L., Swan, J. S., and Nyquist, S. E. (1992) Dolichol and *N*-linked oligosaccharide synthesis in the rat testis. Interaction between Sertoli and spermatogenic cells, evidence for paracrine effects. *Biochem. Cell Biol.* **70,** 496–503
65. Lie, P. P., Xia, W., Wang, C. Q., Mruk, D. D., Yan, H. H., Wong, C. H., Lee, W. M., and Cheng, C. Y. (2006) Dynamin II interacts with the cadherin- and occludin-based protein complexes at the blood–testis barrier in adult rat testes. *J. Endocrinol.* **191,** 571–586
66. Cheng, C. Y., and Mruk, D. D. (2012) The blood-testis barrier and its implications for male contraception. *Pharmacol. Rev.* **64,** 16–64
67. Gilleron, J., Carette, D., Fiorini, C., Dompierre, J., Macia, E., Denizot, J. P., Segretain, D., and Pointis, G. (2011) The large GTPase dynamin2. A new player in connexin 43 gap junction endocytosis, recycling and degradation. *Int. J. Biochem. Cell Biol.* **43,** 1208–1217
68. Nakanishi, A., Abe, T., Watanabe, M., Takei, K., and Yamada, H. (2008) Dynamin 2 cooperates with amphiphysin 1 in phagocytosis in sertoli cells. *Acta Med. Okayama* **62,** 385–391
69. Otsuka, A., Abe, T., Watanabe, M., Yagisawa, H., Takei, K., and Yamada, H. (2009) Dynamin 2 is required for actin assembly in phagocytosis in Sertoli cells. *Biochem. Biophys. Res. Commun.* **378,** 478–482
70. Walensky, L. D., and Snyder, S. H. (1995) Inositol 1,4,5-trisphosphate receptors selectively localized to the acrosomes of mammalian sperm. *J. Cell biol.* **130,** 857–869
71. Pietrobon, E. O., Soria, M., Domínguez, L. A., Monclus Mde, L., and Fornés, M. W. (2005) Simultaneous activation of PLA2 and PLC are required to promote acrosomal reaction stimulated by progesterone via G-proteins. *Mol. Reprod. Dev.* **70,** 58–63
72. Liu, J. P., Powell, K. A., Südhof, T. C., and Robinson, P. J. (1994) Dynamin I is a Ca^{2+}-sensitive phospholipid-binding protein with very high affinity for protein kinase C. *J. Biol. Chem.* **269,** 21043–21050
73. Anantharam, A., Bittner, M. A., Aikman, R. L., Stuenkel, E. L., Schmid, S. L., Axelrod, D., and Holz, R. W. (2011) A new role for the dynamin GTPase in the regulation of fusion pore expansion. *Mol. Biol. Cell* **22,** 1907–1918
74. Larsen, M. R., Graham, M. E., Robinson, P. J., and Roepstorff, P. (2004) Improved detection of hydrophilic phosphopeptides using graphite powder microcolumns and mass spectrometry. Evidence for *in vivo* doubly phosphorylated dynamin I and dynamin III. *Mol. Cell. Proteomics* **3,** 456–465
75. Morita, M., Hamao, K., Izumi, S., Okumura, E., Tanaka, K., Kishimoto, T., and Hosoya, H. (2010) Proline-rich domain in dynamin-2 has a low microtubule-binding activity. How is this activity controlled during mitosis in HeLa cells? *J. Biochem.* **148,** 533–538
76. Ryan, T. A. (2003) Kiss-and-run, fuse-pinch-and-linger, fuse-and-collapse. The life and times of a neurosecretory granule. *Proc. Natl. Acad. Sci.* **100,** 2171–2173
77. Abou-Haila, A., and Tulsiani, D. R. (2003) Evidence for the capacitation-associated membrane priming of mouse spermatozoa. *Histochem. Cell Biol.* **119,** 179–187
78. Faelber, K., Posor, Y., Gao, S., Held, M., Roske, Y., Schulze, D., Haucke, V., Noé, F., and Daumke, O. (2011) Crystal structure of nucleotide-free dynamin. *Nature* **477,** 556–560
79. Altschuler, Y., Barbas, S. M., Terlecky, L. J., Tang, K., Hardy, S., Mostov, K. E., and Schmid, S. L. (1998) Redundant and distinct functions for dynamin-1 and dynamin-2 isoforms. *J. Cell Biol.* **143,** 1871–1881
80. Ferguson, S. M., Brasnjo, G., Hayashi, M., Wölfel, M., Collesi, C., Giovedi, S., Raimondi, A., Gong, L. W., Ariel, P., Paradise, S., O'Toole, E., Flavell, R., Cremona, O., Miesenböck, G., Ryan, T. A., and De Camilli, P. (2007) A selective activity-dependent requirement for dynamin 1 in synaptic vesicle endocytosis. *Science* **316,** 570–574
81. Harper, C. V., Cummerson, J. A., White, M. R., Publicover, S. J., and Johnson, P. M. (2008) Dynamic resolution of acrosomal exocytosis in human sperm. *J. Cell Sci.* **121,** 2130–2135